

Growth of Ga-doped ZnO nanowires by two-step vapor phase method

C. Xu, M. Kim, J. Chun, and D. Kim^{a)}

Physics Department and Electron Spin Science Center, Pohang University of Science and Technology, San 31, Hyoja-Dong, Namku, Kyungbuk 790-784, Republic of Korea

(Received 9 August 2004; accepted 3 February 2005; published online 22 March 2005)

A two-step route is presented to dope Ga into ZnO nanowires and also fabricate heterostructures of Ga-doped ZnO nanowires on ZnO. The content of Ga in ZnO nanowires is about 7 at. % from energy-dispersive x-ray analysis. The single crystal Ga doped ZnO nanowires with the diameter of 40 nm and the length of 300–500 nm are well aligned on the ZnO bulk. The growth direction is along [001]. Raman scattering analysis shows that the doping of Ga into ZnO nanowires depresses Raman E_{1L} mode of ZnO, manifesting that Ga sites in ZnO are Zn sites (Ga_{Zn}). The formation mechanism of $Zn_{1-x}Ga_xO$ nanowires/ZnO heterostructures is proposed. © 2005 American Institute of Physics. [DOI: 10.1063/1.1888035]

Tremendous attention has been paid to ZnO nanowires because of novel physical properties and their potential applications in constructing nanoscale electronic and optoelectronic devices.^{1–7} Recently, Huang *et al.* demonstrated a UV nanolaser at room temperature using highly oriented ZnO nanowire arrays.⁸ ZnO generally reveals *n*-type conduction with a typical carrier concentration of $\sim 10^{17}/\text{cm}^3$,^{9,10} which is smaller than the carrier concentration of $\sim 10^{18}$ to $10^{20}/\text{cm}^3$ in laser diode applications. Hence, the control of carrier concentration remains a significant challenge. Many elements such as Al, Ga, In in group III, Cl, Br and I in group VII have been used as *n*-type dopants in ZnO via vapor phase reaction.^{11–17} Of all elements, Ga is the most effective *n*-type dopant in ZnO since the covalent bond length of Ga–O (1.92 Å) is nearly equal to that of Zn–O (1.97 Å). On the other hand, the tailored nanowires such as Ga, Al, and In doped ZnO nanowires¹⁸ are believed to have more potential for diverse applications, including microelectronics, chemical and biological sensor and diagnosis, energy conversion and storage, light-emitting displays, catalysis, drug delivery, and optical storage.

Semiconductor interfaces are ubiquitous in optoelectronic devices such as light-emitting diodes, quantum-cascade lasers, and transistors. Although a great number of well-developed techniques for the fabrication of thin film heterojunctions are available,¹⁹ an effective route to one-dimensional heterojunction remains challenging; especially, hetero-nanostructures with nearly the same lattice structure (excellent lattice match) will be demanded in practicable applications.

In this letter, we present a two-step vapor phase route to fabricate Ga-doped ZnO nanowires on ZnO bulk or film by using GaN as the mediator. Scanning electronic microscope (SEM), transmission electronic microscope (TEM) and Raman scattering were employed to characterize the as-grown nanowires. We discuss Raman scattering of $Zn_{1-x}Ga_xO$ nanowires. In addition, we propose the formation mechanism of Ga-doped ZnO nanowires on ZnO.

An alumina boat containing the mixture of GaN powder (Aldrich, 99.99%), Zn, and $Zn(\text{CH}_3\text{COO})_2 \cdot 2\text{H}_2\text{O}$ was kept

in the center of a quartz tube placed horizontally in a tubular furnace. The (0001) sapphire substrates were placed downstream from the boat. The distance between the boat and substrates was 300 mm. The base vacuum was kept at 200 mTorr. The powder was heated up to 950 °C at the rate of 15 °C/min with a flow of NH_3 (10 sccm) and Ar (80 sccm). NH_3 was then turned off and air was momentarily purged into the system, which was kept heating to 1050 °C and maintained for 160 min. The system was then cooled down to ambient temperature, and white wool-like products were found on the substrates.

The as-prepared nanowires were investigated by x-ray diffraction (XRD, Rigaku D/max-rB Cu $K\alpha$). The morphology and size distribution of the nanowires were characterized using SEM (HitachiH-8010) equipped with energy-dispersive x-ray (EDX) spectroscopy and TEM (Hitachi H-800). High-resolution TEM (HRTEM) equipped with EDX, and selected area electron diffraction (SAED) analysis was performed with JEOL-2010. The Raman backscattering measurements were performed at room temperature using a Spex 1403 Raman scattering spectrometer and a 200 mW Ar⁺ laser at 488 nm as the excitation source.

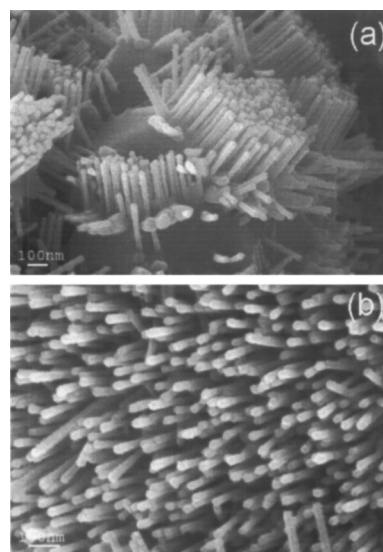


FIG. 1. (a) SEM image of the nanowires grown on a sapphire substrate. (b) Magnified SEM image at a different viewing angle.

^{a)} Author to whom correspondence should be addressed; electronic mail: kimd@postech.ac.kr

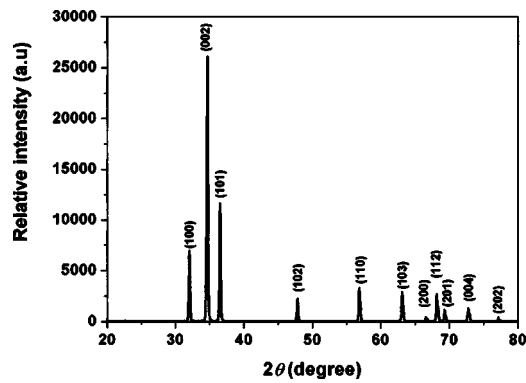


FIG. 2. XRD of Ga-doped ZnO nanowires.

Typical SEM images of the nanowires grown on sapphire substrates are shown in Figs. 1(a) and 1(b). Figure 1(a) shows the nanowires grown on the ZnO bulk. The diameter of the nanowires is uniform and about 40 nm. The length is about 300–500 nm with an aspect ratio of nearly 10:1, which is determined by the SEM image. The nanowires in clusters are well aligned on the surface of the bulk. According to EDX (attached to SEM) analyses, the bulk is composed of Zn and O only, and the atomic ratio of Zn to O is 61:39. The nanowires consist of Zn, O, and Ga; the atomic ratio is 50:46:4. The atomic ratio of Zn to Ga is 93:7. Figure 1(b) reveals the SEM image of enlarged aligned nanowires. The diameters of the nanowires are uniform, the tips are conical, and no droplets are observed.

Figure 2 illustrates XRD of the as-prepared sample. The diffraction peaks are quite similar to those of a bulk ZnO, which can be indexed as the hexagonal wurtzite structure ($a=3.18 \text{ \AA}$, $c=5.18 \text{ \AA}$). No typical diffraction peak corresponding to Ga or Ga compound impurity phases is observed. The strong intensities of the peaks relative to the background delineate that the nanowires are well crystallized. Different from Zn bulk, the strongest peak in the nanowires is (002) rather than (110), implying that the nanowires have a preferred orientation of [001].

Figure 3(a) depicts the typical bright-field TEM image of a Ga-doped ZnO nanowire. The diameter of the nanowire is about 50 nm. The SAED (the upper inset) demonstrates that the nanowire (as indicated by the arrow) is a single crystallite. The indexed diffraction spots confirm that it is hexagonal ZnO with its growth direction being along [001]. EDX attached to TEM results (the lower inset) indicate that the nanowire consists of Zn, O, and Ga with the atomic ratio of

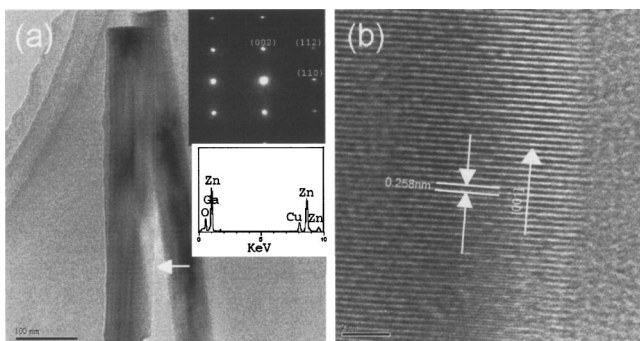


FIG. 3. (a) TEM image of a nanowire grown on the sapphire substrate. The upper inset is SAED; the lower inset is EDX. (b) HRTEM of the corresponding nanowire.

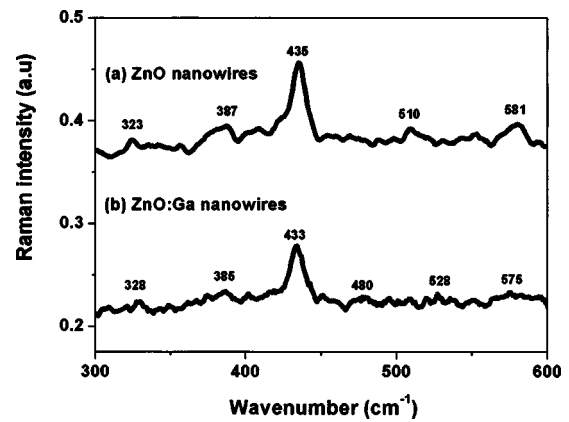


FIG. 4. Raman spectrum of (a) undoped ZnO nanowires grown on a silica substrate and (b) Ga-doped ZnO nanowires/ZnO grown on a sapphire substrate. The excitation was done by 488 nm laser line.

50:44:6. Different areas of a single nanowire and dozens of nanowires have been analyzed by EDX. The results show that some areas in ZnO nanowires are heavily doped with Ga and others relatively lightly doped. Figure 3(b) reveals a HRTEM of the corresponding nanowire. The clear fringes with a spacing of 0.258 nm correspond to the (002) plane of hexagonal ZnO.

Raman scattering is sensitive to the microstructure of nanosized materials. It is also used here to clarify the structure of ZnO:Ga nanowires. Figure 4(a) shows the Raman spectrum of undoped ZnO nanowires (grown on an oxidized Si wafer in a separate experiment) under the excitation at 488 nm laser light. The peaks at 323, 387, 435, and 581 cm^{-1} are assigned to $E_{2H}-E_{2L}$, A_{1T} , E_{2H} and E_{1L} mode of the host ZnO modes,^{20,21} respectively. The broad peak around 510 cm^{-1} can be assigned to the contribution from nanostructures of Si such as nanoparticles in SiO_x ($X < 2$) matrix. Recent works by Khriachtchev *et al.* and Zhang *et al.*²² show that the well-known Raman peak at 520 cm^{-1} from crystalline Si bulk shifts to the region of 510–518 cm^{-1} in the case of Si nanostructures. The observation of the broad peak over the region of 510–518 cm^{-1} in our case indicates that the silica substrate used in the present experiments may contain nanostructures of silicon such as nanoparticles. Figure 4(b) shows a typical Raman spectrum of ZnO:Ga nanowires grown on a sapphire substrate. The peaks at 328, 385, 433, and 575 cm^{-1} are assigned to $E_{2H}-E_{2L}$, A_{1T} , and E_{2H} and A_{1L} of the bulk ZnO modes. The peak at 480 cm^{-1} may be attributed to the contribution from sapphire substrate.²³ As a comparison with the Raman spectrum of undoped ZnO nanowires, the peak at 581 cm^{-1} of ZnO is depressed and hardly observed in ZnO:Ga nanowires, indicating Ga sites at Zn site,²⁴ consistent with the observation of Ga-doped ZnO film.²⁵ This will be helpful in increasing the electron carrier concentration since Ga has the nature of donor. In the case of co-doping Ga and N into ZnO films,²⁶ the enhancement of peak at 580 cm^{-1} of ZnO has been observed because of the acceptor of co-doping Ga and N. The additional peak at 528 cm^{-1} is not well understood. In Sb-doped ZnO film, the similar peak at 531 cm^{-1} has also been observed,²⁵ and related to the individual dopants.

The structural information on Ga-doped ZnO nanowires/ZnO by various analytical techniques mentioned above suggests the following formation mechanism of Ga-doped ZnO nanowires, as depicted in Fig. 5(a).

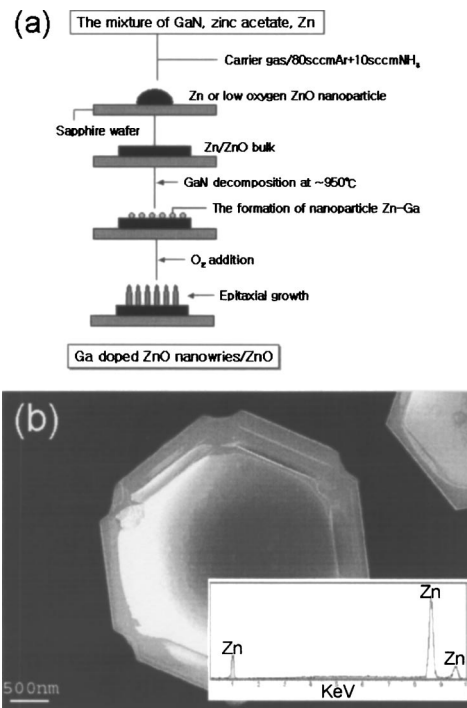


FIG. 5. (a) Formation mechanism of Ga-doped ZnO nanowires. (b) SEM image of a hexagonal Zn particle formed below 700 °C, the inset is for EDX.

In the first step where the system temperature increases and reaches the melting point of Zn (~ 419 °C), in low oxygen pressure, Zn particles evaporated or oxygen-deficient ZnO formed due to residual oxygen deposit onto the sapphire. The additional separate experiment was done below 700 °C without the momentary injection of air to observe what happens in low temperature phase. The results shown in Fig. 5(b) disclose the formation of particles. EDX analysis indicates they are Zn and oxygen-deficient ZnO particles [the inset in Fig. 5(b)]. In the case of (0001) sapphire substrate, ZnO has three-dimensional growth features as well-faceted hexagons [Fig. 5(b)]; moreover, SEM indicates that steps exist on the facets. These features could be attributable to a high interfacial energy associated with the ZnO on sapphire due to large lattice mismatch (16.8%) between sapphire and ZnO, a high surface mobility of Zn adatom, and a substantial desorption of Zn.¹⁰ Note that ammonia is also favorable to eliminate oxygen trace from the system leakage and make the ZnO grow in low oxygen atmosphere. At an elevated temperature, such particles merge to become bulk.

In the second step where the temperature reaches 950 °C, GaN begins to decompose into Ga and N₂, Ga and Zn form Zn-Ga alloy nanoparticles, which act as nucleation sites. The abrupt and momentary introduction of air directly oxidizes the nucleation sites and meanwhile produces more new nucleations¹⁰ on the facets of ZnO. Finally, the nucleation sites grow epitaxially and form well-aligned Ga-doped ZnO nanowires on ZnO. Hence, the hetero-nanostructure of Zn_{1-x}Ga_xO nanowires on ZnO on a sapphire substrate is produced. This formation mechanism is important in a point of view for the fabrication of high quality ZnO-based heterostructures, superlattice, and quantum wells.

In summary, a route is presented to fabricate Ga-doped ZnO nanowires on ZnO on a sapphire substrate. The content of Ga in ZnO nanowires is about 7 at. % from EDX analysis. The single crystal Ga-doped ZnO nanowires are well aligned on the ZnO bulk with a diameter of 40 nm and a length of 300–500 nm. The growth direction is along [001]. The Raman E_{1L} mode of ZnO is depressed in Ga-doped ZnO nanowires, manifesting that Ga sites in ZnO are Zn sites (Ga_{Zn}). The formation mechanism of Ga-doped ZnO nanowires on ZnO is described. This two-step method can be extended to the preparation of other oxide heterojunctions.

The authors appreciate financial support in part from electron Spin Science Center (eSSC) funded by the Korean Science and Engineering Foundation (KOSEF), and from the Brain Korea 21 Project in 2004 funded by the Korean Research Foundation.

- ¹W. Z. Li, S. S. Xie, L. X. Qian, B. H. Chang, B. S. Zou, W. Y. Zhou, A. Zhao, and G. Wang, *Science* **274**, 1701 (1996).
- ²S. S. Fan, M. G. Chapline, N. R. Franklin, T. W. Tomblere, A. M. Cassell, and H. J. Dai, *Science* **283**, 512 (1999).
- ³Z. F. Ren, Z. P. Huang, D. Z. Wang, J. G. Wen, J. W. Xu, J. H. Wang, L. E. Calvet, J. Chen, J. F. Klemic, and M. A. Reed, *Appl. Phys. Lett.* **75**, 1086 (1999).
- ⁴L. C. Qin, D. Zhou, A. R. Krauss, and D. M. Gruen, *Appl. Phys. Lett.* **72**, 3437 (1998).
- ⁵S. H. Tsai, C. W. Chao, C. L. Lee, and H. C. Shih, *Appl. Phys. Lett.* **74**, 3462 (1999).
- ⁶C. Bower, W. Zhu, S. Jin, and O. Zhou, *Appl. Phys. Lett.* **77**, 830 (2000).
- ⁷C. Bower, O. Zhou, W. Zhu, D. J. Werder, and S. H. Jin, *Appl. Phys. Lett.* **77**, 2767 (2000).
- ⁸M. H. Huang, S. Mao, H. Feik, H. Yan, Y. Wu, H. Kind, E. Weber, R. Russo, and P. Yang, *Science* **292**, 1897 (2001).
- ⁹S. Bethke, H. Pan, and B. Wessels, *Appl. Phys. Lett.* **52**, 138 (1988).
- ¹⁰S. Choopun, R. D. Vispute, W. Woch, A. Balsamo, R. P. Sharma, T. Venkatesan, A. Iliadis, and D. C. Look, *Appl. Phys. Lett.* **75**, 3947 (1999).
- ¹¹D. C. Reynolds, D. C. Look, and B. Jogai, *Solid State Commun.* **99**, 873 (1996).
- ¹²D. M. Bagnall, Y. F. Chen, M. Y. Shen, Z. Zhu, T. Goto, and T. Yao, *Appl. Phys. Lett.* **70**, 2230 (1997).
- ¹³D. Song, A. G. Aberle, and J. Xia, *Surf. Sci.* **195**, 291 (2002).
- ¹⁴T. Aoki, Y. Hatanaka, and D. C. Look, *Appl. Phys. Lett.* **76**, 3275 (2000).
- ¹⁵K. Minegishi, Y. Koiwai, Y. Kikuchi, K. Yano, M. Kasuga, and A. Shimizu, *Jpn. J. Appl. Phys., Part 2* **36**, L1453 (1997).
- ¹⁶H. J. Ko, Y. F. Chen, S. K. Hong, H. Wenisch, T. Yao, and D. C. Look, *Appl. Phys. Lett.* **77**, 3761 (2000).
- ¹⁷A. H. Jayatissa, *Semicond. Sci. Technol.* **18**, L27–L30 (2003).
- ¹⁸J. Zhong, S. Muthukumar, Y. Chen, Y. Lu, H. M. Ng, W. Jiang, and E. L. Garfunkel, *Appl. Phys. Lett.* **83**, 3401 (2003).
- ¹⁹D. M. Bagnall, Y. F. Chen, Y. F. Zhu, Z. Yao, T. Koyama, S. Shen, and M. Y. Goto, *Appl. Phys. Lett.* **70**, 2230 (1997).
- ²⁰M. Rajalakshmi, A. K. Arora, B. S. Bendre, and S. Mahamuni, *J. Appl. Phys.* **87**, 2445 (2000).
- ²¹T. C. Damen, S. P. S. Porto, and B. Tell, *Phys. Rev.* **142**, 570 (1966).
- ²²L. Khriachtchev, M. Rasanen, S. Novikov, and L. Pavesi, *Appl. Phys. Lett.* **85**, 1511 (2004); L. Khriachtchev, S. Novikov, and J. Lahtinen, *J. Appl. Phys.* **92**, 5856 (2002); S. Zhang, W. Ding, Y. Yan, J. Qu, B. Li, L. Li, K. Yue, and D. Yu, *Appl. Phys. Lett.* **81**, 4446 (2002).
- ²³A. S. Barker, Jr., *Phys. Rev.* **132**, 1474 (1963).
- ²⁴M. H. Yoon, S. H. Lee, H. L. Park, H. K. Kim, and M. S. Jang, *J. Mater. Sci. Lett.* **21**, 1703 (2002).
- ²⁵C. Bundesmann, N. Ashkenov, M. Schubert, D. Spemann, T. Butz, E. M. Kaidashev, M. Lorenz, and M. Grundmann, *Appl. Phys. Lett.* **83**, 1974 (2003).
- ²⁶N. Hasuike, H. Fukumura, H. Harima, K. Kisoda, H. Matusi, H. Saeki, and H. Tabata, *J. Phys.: Condens. Matter* **16**, S5807 (2004).